Dual-Segment Three-Phase PMSM With Dual Inverters for Leakage Current and Common-Mode EMI Reduction

Zewei Shen, *Student Member, IEEE*, Dong Jiang, *Senior Member, IEEE*, Tianjie Zou, *Student Member, IEEE*, and Ronghai Qu, *Fellow, IEEE*

***Abstract*—In a motor drive system, the inverter working in discrete and impulse states generates a common-mode voltage (CMV) at the terminal of the stator winding neutral point. The high-frequency CMV can induce a leakage current and a common-mode (CM) electromagnetic interference (EMI), which are potential threats to personal safety and system stability. The conventional single three-phase inverter is found to be powerless in eliminating the CMV, while the two paralleled inverters can effectively eliminate the CMV theoretically, but the three coupled inductors (CIs) should be added to the motor drive system which reduces the power density and efficiency of the system. A novel method, which associates a specially designed dual-segment three-phase motor with the CMV elimination modulation algorithm, can be utilized to cancel the extra CIs without degrading the function of the leakage current and the CM EMI suppression. The design of the dual-segment three-phase permanent magnet synchronous machine is introduced, with identical back electromotive forces for two groups of windings but with little magnetic coupling between them. Simulation and experimental results are provided to verify the validity of the proposed method in CM-related reduction and CI cancellation. Compared with the zero-CM pulsewidth modulation for paralleled inverters proposed in a previous work, the proposed dual-segment three-phase motor drive can achieve a better power density by removing the CIs.**

***Index Terms*—Common mode (CM), coupled inductors (CIs), dual-segment three-phase machine, electromagnetic interference (EMI).**

NOMENCLATURE

Acronyms

PWM	Pulsewidth modulation.
VSI	Voltage source inverter.
CMV	Common-mode voltage.
CMC	Common-mode current.
CI	Coupled inductor.

Manuscript received June 5, 2018; accepted August 9, 2018. Date of publication August 19, 2018; date of current version April 20, 2019. This work was supported by the National Natural Science Foundation of China under Project 51607077. Recommended for publication by Associate Editor T. Shimizu. *(Corresponding author: Dong Jiang.)*

The authors are with the State Key Laboratory of Advanced Electromagnetic Engineering and Technology, School of Electrical and Electronic Engineering, Huazhong University of Science and Technology, Wuhan 430074, China (e-mail:

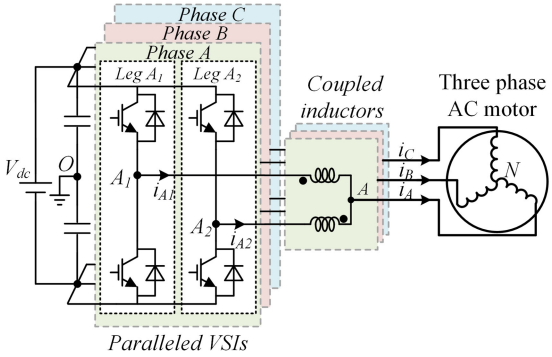

Fig. 1. System configuration of a paralleled inverter-fed three-phase ac motor with CIs.

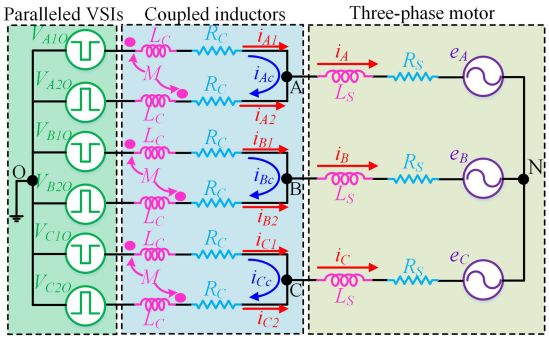

Fig. 2. Simplified equivalent circuit model of the paralleled inverter system with a three-phase motor.

the conventional two-level three-phase VSI can only reduce the CMV but cannot eliminate it with general modulation algorithm, which makes the CM EMI filter inevitable for the motor drive system. To deal with the problem of insufficient freedom, the modified topology can be utilized to realize the CMV elimination effect. In [15] and [16], the three-level and multilevel inverters cooperating with particular PWM schemes are utilized to eliminate the CMV in typical three-phase loads, but with the tradeoff of current ripples and total harmonic distortion (THD) deterioration. In [17], the dual-winding stator configuration driven by a dual inverter, which provides even switching state combinations, is implemented for CMV cancellation, and it has been proved that a simplified structure with a nine-switch inverter has a similar CMV elimination effect [18], [19].

Similarly, the dual inverter with paralleled manner is a popular structure, which not only has the ability to increase the power rating of the system [20] but also the possibility to suppress or even eliminate the CMV in an ideal condition [21], [22]. The system configuration of paralleled inverters feeding a three-phase ac motor is shown in Fig. 1. The paralleled manner realization is contributed to the three extra coupled inductors (CIs), which limit the circulating current in the paralleled phase-legs. Compared with other CMV elimination schemes' topology [15]–[19], though the proposed zero common-mode voltage (ZCMV) PWM scheme proposed in [22] has the potential to cancel out the big CM choke, the added three CIs not only increase the volume and weight of the system but also make the whole system complex. Meanwhile, in large power applications, the dc-bus voltage is usually high and the switching frequency is often limited to hundreds of Hz or several kHz, which obviously enlarges the circulating current [23] and leads to the design and manufacture of a huge CI that loses the superiority of the CM choke cancellation effect or may reduce the power density of the system finally.

The pivotal role of a CI is to provide the suitable inductance in the circulating path to restrain the circulating current. Actually, there exists another kind of inductor in the ASD system, i.e., the stator inductor of the motor, which has the potential to offer the so-called "suitable inductance." In order to integrate the stator inductor with the function of circulating current suppression, a special motor should be designed to work with the dual inverter. Under this condition, the motor ASD system consists of a dual inverter and the specially designed motor without the extra CIs, which not only simplify the ASD system but also increase the power density of the whole system. This paper gives a detailed introduction of the overall method for the ZCMV scheme with the specially designed motor to realize the CMV-related problem mitigation.

The rest of this paper is organized as follows. Through the analysis of different CMV reduction modulation schemes, the principle of CI elimination is introduced with theoretical analysis in Section II. To satisfy the demand of the stator winding and for the back electromotive force (EMF) to cooperate with the selected ZCMV scheme, a special dual-segment three-phase permanent magnet synchronous machine (PMSM) is introduced in Section III, which includes the design result, an approximate mathematical model, and the corresponding control strategy. In Section IV, using simulations, the proposed structure utilizing the ZCMV method is first tested and compared with other schemes; in particular, a fair and detailed comparison is made with the already proposed paralleled inverter with the CI scheme. The detailed experimental results are presented in Section V, which prove the validity and superiority of the proposed method. Conclusions are provided in Section VI.

II. Structure Optimization of a Motor Drive System

A. Analysis of Different CMV Reduction Modulation Schemes

Based on the system structure shown in Fig. 1, a simplified equivalent circuit model of the system can be set up, as shown in Fig. 2, where V_{A1O}, V_{A2O}, V_{B1O}, V_{B2O}, V_{C1O}, and V_{C2O} are the pole voltages of six phase-legs, which switch between the values of $V_{\rm dc}/2$ and $-V_{\rm dc}/2$, with a dc-link voltage of $V_{\rm dc}$, i_{A1}, i_{A2}, i_{B1}, i_{B2}, i_{C1}, and i_{C2} are the phase-leg currents, i_A, i_B, and i_C are the output phase currents, and $i_{\rm Ac}$, $i_{\rm Bc}$, and $i_{\rm Cc}$ are the three-phase circulating currents flowing through CIs. For each CI, L_c, M, and R_c are the main inductance, mutual inductance, and resistance, respectively. As for the three-phase motor, each phase can be simplified as a stator inductor, a stator resistance, and a back EMF connected in series, which are represented by L_S, R_S, and $e_{\rm X}$ $(X = A, B, C)$, respectively.

Considering the symmetry of a CI, the phase voltage (taking the dc-side middle-point as the reference) can be deduced using the principle of circuit simplification as follows:

$$V_{XO} = \frac{1}{2}\left(V_{X1O} + V_{X2O}\right), \quad (X = A,\ B, C). \tag{1}$$

In this case, when the paralleled phase-legs output the same pole voltages, whether $V_{\rm dc}/2$ or $-V_{\rm dc}/2$, the combined output phase voltage of the CI keeps the identical states. When the paralleled phase-legs output the opposite pole voltages, the combined output phase voltage of the CI is zero and the circulating current obviously varies under this condition. Thus, the essence of paralleled inverters with CIs is the three-level inverter, and the critical role of the CI is to provide the function of different switching state combinations.

In addition, with the symmetry of motor stator windings, the CMV in the conventional three-phase motor can be deduced, which is the instantaneous average value of three phase voltages. Consequently, the CMV generated by the paralleled inverters is given by

$$\begin{aligned} V_{\rm cm} &= \frac{1}{3}\left(V_{AO}+V_{BO}+V_{CO}\right) \\ &= \frac{1}{3}\left[\frac{1}{2}\left(V_{A1O}+V_{A2O}\right)+\frac{1}{2}\left(V_{B1O}+V_{B2O}\right)\right. \\ &\quad \left.+\frac{1}{2}\left(V_{C1O}+V_{C2O}\right)\right] \\ &= \frac{1}{6}\left(V_{A1O}+V_{A2O}+V_{B1O}+V_{B2O}+V_{C1O}+V_{C2O}\right). \end{aligned} \tag{2}$$

More combinatorial CMV values can be realized by increasing the number of phase-legs to six, especially the zero state, which cannot be realized in a single three-phase inverter-driven system.

In order to restrain the circulating current and reduce the volume of CI in paralleled inverters, a high-frequency technology, which requires the paralleled phase-legs to maintain an identical average pole voltage in every switching cycle, should be implemented. To satisfy this requirement, Jiang *et al.* [22] have introduced three different modulation schemes, including the conventional SVPWM, the SVPWM with half switching cycle interleaving, and ZCMV schemes, wherein the effects of CMV reduction are different. The basic principle of reference voltage synthesis for SVPWM is depicted in Fig. 3(a). In the conventional SVPWM scheme, the corresponding phase-legs are driven by identical PWM signals, which lead to identical currents in the paralleled phase-legs under ideal condition. In this case, only the phase voltage switches between $V_{\rm dc}/2$ and $-V_{\rm dc}/2$. In addition, since the same zero voltage vectors (000, 111) are utilized simultaneously, the CMV has a maximum peak value of $\pm V_{\rm dc}/2$, as shown in Fig. 3(b). In order to reduce the CMV, the extra interleaving strategy for paralleled inverters can be utilized, as shown in Fig. 3(c). With half switching cycle interleaving, the voltage vectors' combination can be changed. More importantly, the CMV can be reduced to $\pm V_{\rm dc}/6$, with the effect of canceling out different zero voltage vectors. The interleaving manner, however, cannot eliminate the CMV, and the impairment of the motor caused by the CMV still exists.

Fig. 4 shows the characteristic of the ZCMV scheme, including the sector division and PWM signals distribution. From Fig. 4(a), it can be seen that the sector division of the ZCMV has a 30° lag when compared with the SVPWM, and the six active

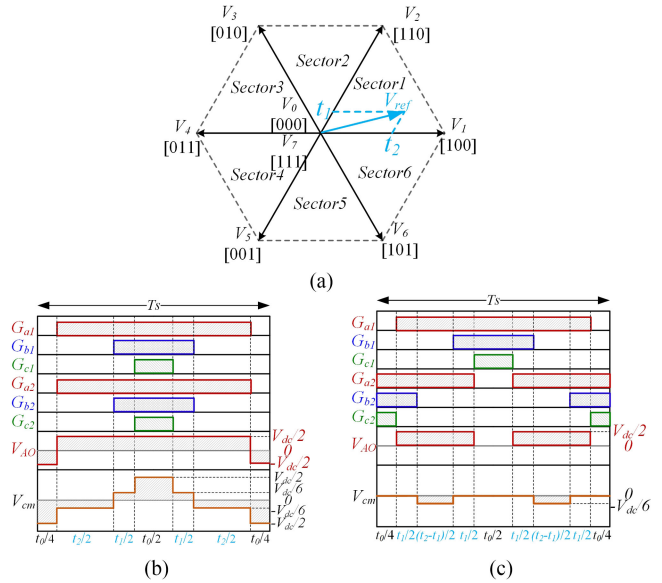

Fig. 3. Conventional modulation schemes for paralleled inverters. (a) Principle of reference voltage synthesis with space voltage vectors for the SVPWM. (b) Conventional SVPWM scheme. (c) SVPWM with half switching cycle interleaving scheme.

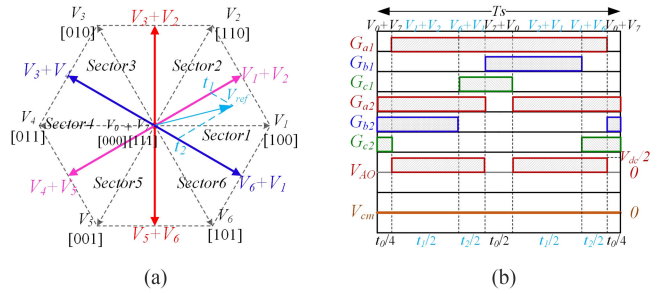

Fig. 4. Principle of the ZCMV scheme for paralleled inverters. (a) Reference voltage synthesis. (b) PWM scheme in sector 1.

voltage vectors are made up of basic adjacent voltage vectors. In each sector, the reference voltage can be generated by two adjacent active paralleled voltage vectors with common paralleled zero voltage vectors. The principle of reference voltage vector synthesis is similar to that of the SVPWM, wherein the active time for two adjacent paralleled voltage vectors is t_1 and t_2 in each switching cycle, with the remaining zero vector time being t_0. The PWM signals, phase voltage, and the CMV in sector 1 are depicted in Fig. 4(b). It can be seen that the PWM signals of phases B and C are artificially changed to be asymmetric so as to align each rising edge and falling edge, which can eliminate the instantaneous CMV pulse and keep the CMV at zero for the whole switching cycle. Thus, the ZCMV scheme has the best CMV suppression effect theoretically. A more detailed principle for this novel modulation scheme can be found in [22].

Though Jiang *et al.* [22] introduced the ZCMV scheme, the CMV suppression effects were tested only with *R–L* loads, not with the object that is of most concern—the ac motor. More importantly, the modulation scheme is only suitable for paralleled inverters, and the use of three bulky CIs inevitably results in the system being more complex than other CMV

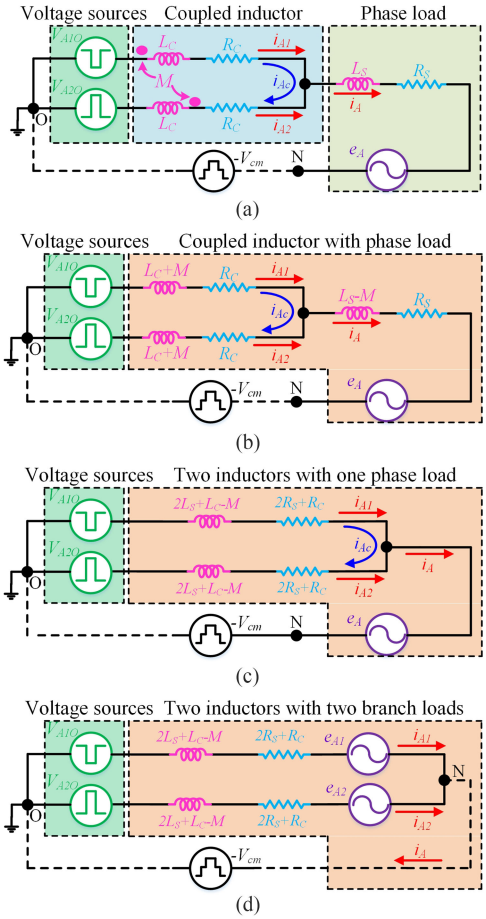

Fig. 5. Process of CI elimination. (a) Original equivalent circuit model of one phase. (b) Equivalent circuit model with CI decoupling. (c) Equivalent circuit model with merging of external inductors and stator inductor. (d) Equivalent circuit model without external inductors.

elimination schemes, such as the three-level CMV elimination scheme directly driving a three-phase motor [15] and the dual-inverter driving a dual three-phase winding motor [17]. In view of the two above-mentioned problems, in the following content, the principle of CI elimination is introduced, which makes the requirement of the motor explicit, and the testing of the ZCMV scheme with the specially designed motor is performed to verify the feasibility and superiority when compared with the conventional paralleled inverters with CIs' scheme.

B. Principle of CI Elimination

In order to deduce the principle of CI elimination and simplify the analysis, two paralleled phase-legs with a single CI and the corresponding phase load are extracted. Considering phase A, for example, the single-phase model can be built, as shown in Fig. 5(a). It can be seen that both the CI and phase load have inductors. The main inductor of the CI limits the circulating current between the paralleled phase-legs caused by the instantaneous pole voltage difference, while the inductor of the phase load is the stator inductance of the motor. If these two inductors can be integrated into one inductor, the simplified system that eliminates CIs can be realized.

Following the above-mentioned idea, Fig. 5(b)–(d) shows the simplified process. Using the circuit decoupling equivalence principle, Fig. 5(b) depicts the equivalent circuit with the CI decoupling. Under this condition, the two inductors $L_c + M$ can be regarded as two external separate inductors inserted into the circulating path to limit the circulating current i_{Ac}, while the inductor $L_S - M$ can be regarded as the new motor stator inductor. Based on the circuit principle of series and parallel transformation, the equivalent circuit model shown in Fig. 5(b) can be further simplified, and the result is shown in Fig. 5(c). Under this circumstance, the external inductor and the stator inductor can be merged to become one inductor with an inductance of $2L_S + L_c - M$, and the merged resistance follows the same law with a value of $2R_S + R_c$. In this case, the combined inductor not only provides the function of circulating current suppression, but it can also be regarded as the stator inductor; thus, the external inductor can be eliminated. Meanwhile, considering the mandatory rule that one stator inductor should have its own back EMF, the back EMF of one phase should be decomposed into two back EMFs and the phase load can be regarded as two branch loads, as shown in Fig. 5(d). The increasing number of stator inductor indicates the changing physical requirement of the motor that one set stator winding should increase to two; hence, the conventional three-phase motor should be modified into a dual three-phase winding motor. In addition, according to the circuit principle, the relationship $e_{A1} = e_{A2} = e_A$ should be satisfied; each homologous stator inductor should, therefore, have an identical back EMF. It should be clarified that though the winding configuration is similar to that in the methods proposed in [17]–[19], the back EMF demand of two homologous stator inductors is different, which eventually makes the modulation algorithm distinct.

Considering the definition of CMV for this special motor, the CMV remains unchanged when compared with (2), while the influence of stator winding modification on the CMV-related problem should be analyzed. In the conventional three-phase motor with a single set of stator winding, taking the main impedance of the CM path in the motor into consideration, the simplified CM equivalent model can be drawn, as shown in Fig. 6(a), where Z_{dg} is the dc-link midpoint grounding impedance, Z_{cable} is the transmission impedance of the cable for each phase, C_{sf} and C_{sr} are the capacitors between the stator winding and motor frame and that between the stator winding and rotor, respectively, for each phase, and C_{rf} represents the entire capacitive coupling between the rotor and motor frame [3]. It should be noted that the high-frequency leakage current is not a conduction current flowing in the stator winding but a displacement current caused by the corresponding stray capacitors [1]. Thus, R_{sf}, R_{sr}, and R_{rf} are not the conductive resistances, but they express the iron-core loss for the high-frequency leakage current physically [24]. The simplified model of the motor bearing consists of the resistor R_b, the switch S_b, and the adjustable capacitor C_b [3]. Owing to the symmetric characteristic of the CM equivalent branch circuit for each phase under ideal condition, it can be easily deduced that the induced motor frame voltage can be restrained to zero with the ZCMV modulation scheme; thus, the leakage current and CM EMIs can also be suppressed.

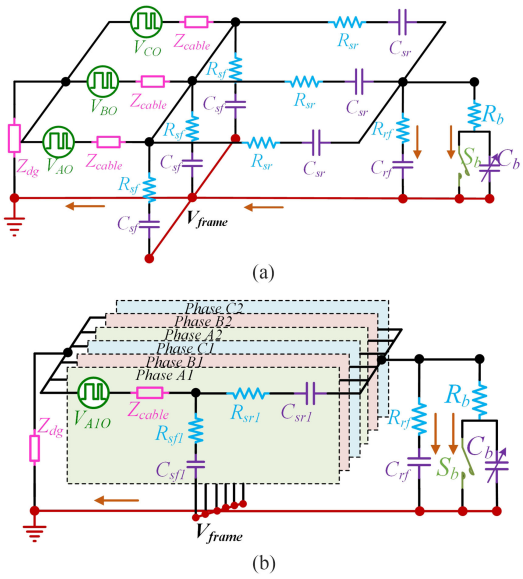

Fig. 6. CM equivalent model comparison for a typical three-phase motor drive system and the dual three-phase motor drive system. (a) Typical three-phase motor drive system. (b) Dual three-phase motor drive system.

Similarly, considering the stray coupling in a dual winding motor, the corresponding CM equivalent model can also be set up, as shown in Fig. 6(b). With the number of stator winding increased, the parasitic coupling branch of the stator winding should also be increased and the corresponding stray parameters that are decided by the coupling area for each phase winding should be changed. Thus, the impedance between the stator winding and motor frame and the impedance between the stator winding and rotor are redefined as C_{sf1}, C_{sr1}, R_{sf1}, and R_{sr1}, respectively. As for the impedance between the rotor and frame, and the bearing model, they are not influenced by the stator winding separation and remain the same. Under this condition, with the symmetric characteristic of the CM circuit, the high-frequency displacement current can cancel out each other, regardless of the increase of the parasitic coupling branch; thus, the leakage current and the CM EMI suppression effect can also be retained under ideal condition.

III. Dual-Segment Three-Phase PM Machine Design and Control Principle

Since the structure of the requested motor is more complicated than the conventional three-phase PMSM, the design and control method should be considered. In this section, the proposed dual-segment three-phase motor design and back EMF test are first implemented; then, the simplified mathematical model of the designed motor is derived; in addition, the relevant sector judging method for the ZCMV scheme is introduced, and the corresponding control block diagram is deduced based on this analysis.

A. Dual-Segment Three-Phase Motor Design and Test

In order to build the motor drive system, a PMSM prototype with two sets of symmetrical three-phase windings has been

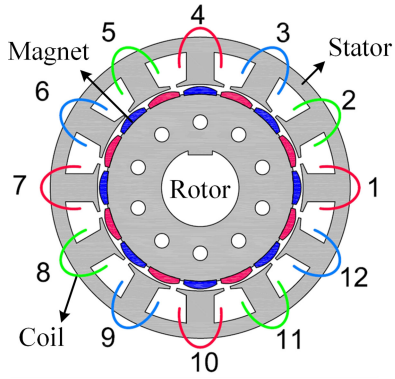

Fig. 7. Sketch of the motor topology.

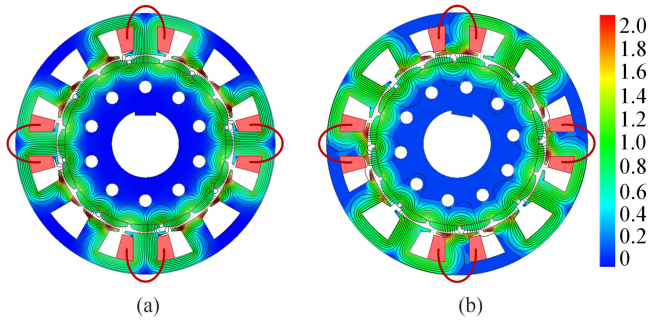

Fig. 8. Flux contour plots of the machine. (a) Open circuit. (b) Rated load.

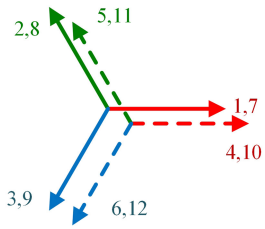

Fig. 9. Star of slots' vector gram.

designed. As shown in Fig. 7, the motor is constructed with a 12-slot stator wound with double-layer nonoverlapping coils. The 8-pole pair permanent magnet (PM) rotor comprises a slot/pole combination of 12/16 together with the stator. According to the classical winding theory of ac machines, the periodicity number of the 12/16 motor is 4.

Fig. 8 shows the finite element analysis (FEA)-based flux contour plots of the motor under open-circuit and rated load conditions, and it can be clearly seen that the flux distribution repeats itself four times along the periphery. Due to this periodicity, the coils can be divided into three groups according to their difference in space vectors, which are shifted by 120° electrical angle. Meanwhile, the four coils in each group can induce a back EMF with exactly the same waveform. Hence, one set of the dual-segment three-phase winding can simply be designed by selecting any two coils from each group to form one phase. Practically, the dual-segment three-phase winding is implemented according to the star of slots plot, as shown in Fig. 9, and the winding is specifically configured as

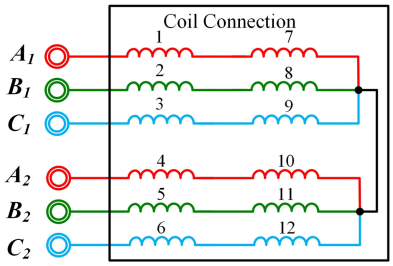

Fig. 10. Connection of two-segment windings.

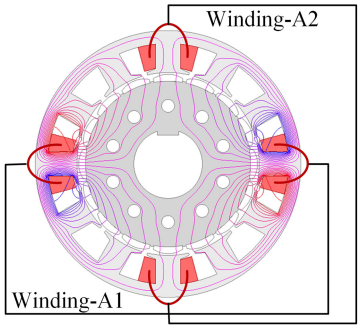

Fig. 11. Armature reaction of the winding A1.

illustrated in Fig. 10. In order to investigate the mutual coupling of corresponding phases from each set of winding with the same back EMF, the armature reaction of the motor is further evaluated through the FEA. As illustrated in Fig. 11, there is only a weak coupling between phases A1 and A2. Besides, the FEA-based calculation results show that the mutual inductance between A1 and A2 is only 0.1372 mH, i.e., ∼11% of the self-inductance of 1.172 mH. Thus, this specially designed motor can prevent the stator inductor from being overly weakened by the mutual inductance of different windings, which is helpful in restraining the increase of current ripples in phase-leg currents.

According to the classical winding theory of ac machines, the periodicity number of the 12/16 motor is 4. According to the optimally designed PMSM scheme, a two-segment prototype PMSM was fabricated. The stator, rotor, and the assembled motor with the testbench are shown in Fig. 12(a) and (b). The two-segment rotor skewing is considered to optimize the output torque and reduce the cogging torque. In addition, the key parameters of the designed PMSM are listed in Table I.

In order to verify the feasibility of the designed motor, the back EMF test is first performed at the rated rotation speed. The results are depicted in Fig. 13(a) and (b). It can be seen that the fundamental electrical period of the back EMF is 7.5 ms, which conforms to the design rated speed. More importantly, the two homologous stator inductors are proved to have nearly identical back EMFs. Considering the fundamental and harmonic voltages in the back EMF, the frequency-domain analysis is performed. It can be seen that the fundamental back EMFs of all stator inductors are close to 33 V, and the harmonics are small enough to be ignored in the motor control process.

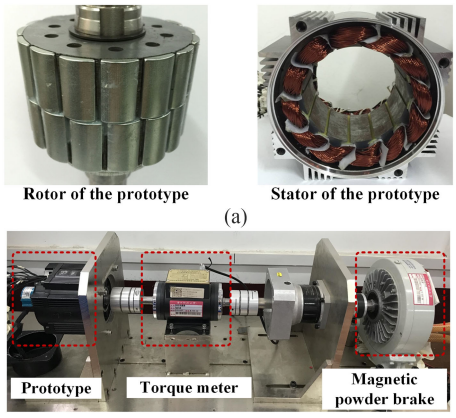

Fig. 12. Motor prototype and testbench. (a) Motor prototype. (b) Testbench.

TABLE I
KEY PARAMETERS OF THE DESIGNED PMSM

Parameters	Value
PM flux linkage	0.023Wb
Stator inductance	1.2mH
Phase resistance	0.2Ω
Rated rotation speed	1000rpm
Rated fundamental frequency	133.3Hz
Rated line voltage	75V
Rated line current	8.5A
Rated torque	8.3Nm

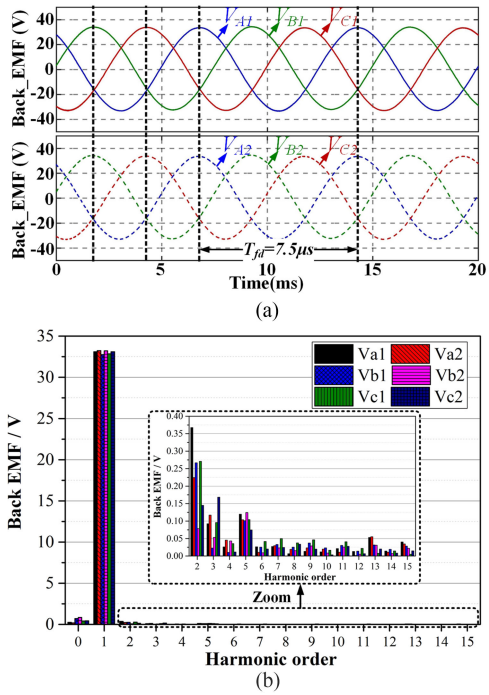

Fig. 13. Test results of the back EMF for a dual-segment motor. (a) Time-domain waveform. (b) Frequency-domain analysis.

B. Mathematical Model for the Dual-Segment Three-Phase Motor

A general dual three-phase motor often consists of two sets of three-phase windings spatially shifted by 30 electrical degrees. In addition, the two sets of stator windings have an obvious magnetic coupling, which adds to the complexity of the mathematic model of the dual three-phase motor and also to the complexity of the control method. In contrast, though the designed dual-segment motor has multiset stator windings, only three phase back EMFs exist in the stator winding sets. More importantly, in the FEA analysis, different sets of phase windings with the same back EMF have little magnetic coupling; hence, the influence of different stator winding sets can be neglected to reduce the complexity of the system. In this case, the modeling of the designed motor can be regarded as a combination of two conventional three-phase motors, and the control method can follow the conventional three-phase ac motor's control method. Thus, ignoring the small magnetic coupling between the two sets of windings, the mathematical model of each set of winding is identical with that of a regular three-phase PM machine, and the flux and voltage equations in the *d–q* reference frame can be written as follows:

$$\begin{bmatrix}\psi_{d1}\\ \psi_{q1}\\ \psi_{d2}\\ \psi_{q2}\end{bmatrix}=\begin{bmatrix}L_{d1}&0&0&0\\ 0&L_{q1}&0&0\\ 0&0&L_{d2}&0\\ 0&0&0&L_{q2}\end{bmatrix}\begin{bmatrix}i_{d1}\\ i_{q1}\\ i_{d2}\\ i_{q2}\end{bmatrix}+\begin{bmatrix}\psi_f\\ 0\\ \psi_f\\ 0\end{bmatrix} \tag{3}$$

$$\begin{bmatrix}U_{d1}\\ U_{q1}\\ U_{d2}\\ U_{q2}\end{bmatrix}=\begin{bmatrix}R_S&0&0&0\\ 0&R_S&0&0\\ 0&0&R_S&0\\ 0&0&0&R_S\end{bmatrix}\begin{bmatrix}i_{d1}\\ i_{q1}\\ i_{d2}\\ i_{q2}\end{bmatrix}+\frac{d}{dt}\begin{bmatrix}\psi_{d1}\\ \psi_{q1}\\ \psi_{d2}\\ \psi_{q2}\end{bmatrix}+\omega_r\begin{bmatrix}-\psi_{q1}\\ \psi_{d1}\\ -\psi_{q2}\\ \psi_{d2}\end{bmatrix} \tag{4}$$

where ψ_{dk}, ψ_{qk}, U_{dk}, U_{qk}, i_{dk}, and i_{qk} ($k = 1, 2$) are the *d–q* axis flux linkages, voltages, and currents, respectively. ψ_f is the flux linkage produced by the PMs, R_S is the stator resistance per phase, and ω_r denotes the electrical angular speed of the rotor. Under this condition, the whole torque is composed of each segment torque of the motor. Considering the characteristic $L_{dk} = L_{qk}$ of this surface-mounted PMSM, the simplified equation for the total torque can be deduced as follows:

$$\begin{aligned}T_e&=\frac{3}{2}p\left[\psi_f\left(i_{q1}+i_{q2}\right)+\left(L_{d1}-L_{q1}\right)i_{d1}i_{q1}\right.\\&\quad\left.+\left(L_{d2}-L_{q2}\right)i_{d2}i_{q2}\right]\\&=\frac{3}{2}p\psi_f\left(i_{q1}+i_{q2}\right).\end{aligned} \tag{5}$$

With above-mentioned analysis, for the designed dual-segment three-phase motor, the output torque is decided by the summation of two *q*-axis currents in each set of stator windings. As for other aspects of the control process, they follow the conventional control principle and are similar to those of the conventional three-phase motor.

C. Sector Judging Method of the ZCMV Modulation Scheme

In the closed-loop control process, the key step is to accurately judge the sector in real time. With the research of the inherent correlation between carrier-based PWM and conventional SVPWM in two-level inverters, the reduced computational method without sector judgement can be used to realize SVPWM effect by injecting the real-time CM-modulated signal into the sinusoidal modulation wave [25]. As for the ZCMV scheme, the pivotal phaseshift process for PWM signals is decided by the sector [22]. However, regardless of whether the average or instantaneous CMV is eliminated, the CM injection method cannot be implemented in this case, and a novel sector judging method should be developed.

For the ZCMV scheme, the reference output average voltage of six phase-legs can be obtained from the *d–q* current controllers by inverse Park transform as follows:

$$\begin{cases}V_{a1}=V_{a2}=d_a^*\cdot V_{\rm dc}/2\\ V_{b1}=V_{b2}=d_b^*\cdot V_{\rm dc}/2\\ V_{c1}=V_{c2}=d_c^*\cdot V_{\rm dc}/2\end{cases} \tag{6}$$

where d_a^*, d_b^*, and d_c^* are the quasi-duty cycles varying from -1 to 1. Considering the effect of CMV elimination for this scheme, we have

$$\begin{aligned}V_{\rm cm}&=\frac{1}{6}\left(V_{A1O}+V_{A2O}+V_{B1O}+V_{B2O}+V_{C1O}+V_{C2O}\right)\\&=\frac{V_{\rm dc}}{3}\left(d_a^*+d_b^*+d_c^*\right)=0.\end{aligned} \tag{7}$$

Thus, the summation of three quasi-duty cycles must be zero in every switching cycle, and this potential constraint can be utilized to judge the sector. Actually, two quasi-duty cycles with the same sign can be used to determine the sector and all six combinations of the three quasi-duty cycles can uniquely determine six sectors. For example, when d_b^* and d_c^* are both negative, d_a^* must be positive and the sector is 1. At the same time, the synthesized voltage vector's effective time t_1, t_2, and the remaining time t_0 can be calculated as follows:

$$\begin{cases}t_1=-d_c^*\\ t_2=-d_b^*\\ t_0=1-d_a^*.\end{cases} \tag{8}$$

With t_1, t_2, and t_0, the PWM signal of six phase-legs can be obtained, according to the modulation algorithm. Similar to the above-mentioned analysis, all sectors' judging condition and time-segment calculation are as listed in Table II. According to Table II, the sector can be judged and the PWM signals for the whole fundamental period can be obtained.

With the aforementioned analysis, the control block diagram of the system can be set up, as shown in Fig. 14. The control strategy is similar to the normal field-oriented control for a three-phase motor. The different parts are the sector judging method and the modulation algorithm. In addition, the current

TABLE II
SECTOR JUDGING CONDITION AND TIME-SEGMENT CALCULATION OF THE ZCMV PWM ALGORITHM

	Sector judging condition	Time segment calculation
sector 1	$d_b^*<0, d_c^*<0$	$t_1=-d_c^*, t_2=-d_b^*, t_0=1-d_a^*$
sector 2	$d_a^*>0, d_b^*>0$	$t_1=d_b^*, t_2=d_a^*, t_0=1+d_c^*$
sector 3	$d_a^*<0, d_c^*<0$	$t_1=-d_a^*, t_2=-d_c^*, t_0=1-d_b^*$
sector 4	$d_b^*>0, d_c^*>0$	$t_1=d_c^*, t_2=d_b^*, t_0=1+d_a^*$
sector 5	$d_a^*<0, d_b^*<0$	$t_1=-d_b^*, t_2=-d_a^*, t_0=1-d_c^*$
sector 6	$d_a^*>0, d_c^*>0$	$t_1=d_a^*, t_2=d_c^*, t_0=1+d_b^*$

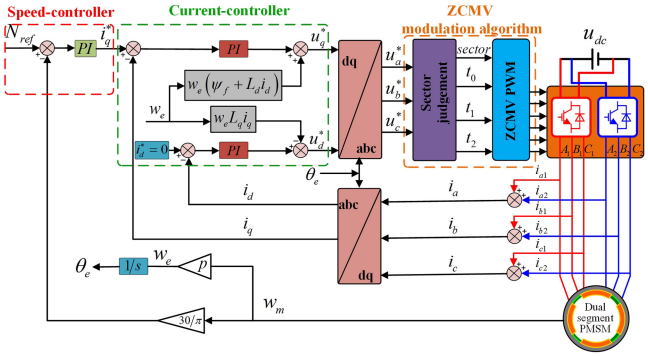

Fig. 14. Control block diagram of the system.

feedback control, which requires the sampling of six phase-legs' currents, should combine the corresponding phase-legs' currents into one phase before adopting the inverse Park and Clark transformations ($abc/\alpha\beta$ and $\alpha\beta/dq$).

IV. SIMULATION RESULTS

In order to test the effect of the proposed dual-segment motor controlled by the ZCMV scheme and to perform a fair comparison with other methods, a simulation model based on MATLAB/Simulink software has been developed. Fig. 15 shows the different stator winding configurations of the dual-segment three-phase motor for different structures, in which the first configuration is based on paralleled inverters with a CI structure, as shown in Fig. 15(a), while the other stator winding configuration is the proposed dual inverter with a dual stator winding structure, as shown in Fig. 15(b).

Based on the designed parameters for the dual-segment three-phase motor, the suitable simulation parameters can be decided, as given in Table III. The simulation is done with a dc-link voltage of 75 V and at 10-kHz switching frequency. The main parameters for the CI, which include the main inductance and the coupling coefficient, can be extracted from the actual CI to simulate the actual condition. Moreover, the main CM loop, which neglects the influence of bearing for the leakage current, i.e., the stray circuit between the stator winding and the motor frame, is added in the simulation model to test the characteristic of the leakage current for different modulation schemes. The stray capacitor for each phase winding and motor frame can be extracted by the *LCR* meter KEYSIGHT E4980AL, while

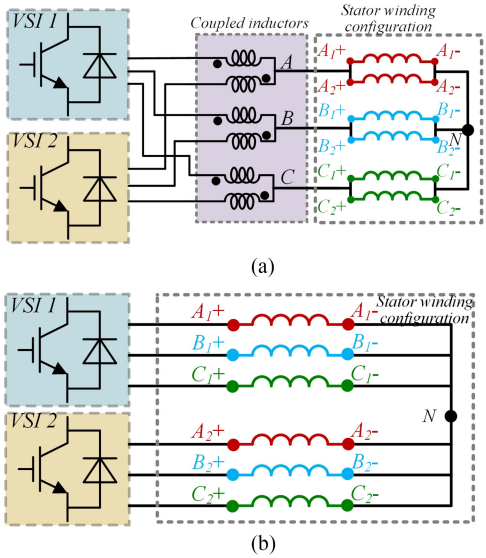

Fig. 15. Different stator winding configurations. (a) Paralleled inverters with a CI. (b) Dual inverter with a dual winding.

TABLE III
SIMULATION PARAMETERS

Symbol	Parameters	Value
V_{dc}	DC link voltage	75V
f_s	Switching frequency	10kHz
L_c	Main inductance of CI	0.52mH
M	Coupling coefficient of CI	0.92
L_s	Stator inductance	1.2mH
N_{ref}	Reference rotation speed	375rpm
f_0	Fundamental electrical frequency	50Hz
i_d	D-axis reference current	0
i_q	Q-axis reference current	8.5A
T_e	Reference torque	4.15Nm
C_{sf}	Stray capacitor for each phase winding and motor frame	0.15nF
R_{sf}	Equivalent resistor for each phase winding and motor frame	100Ω

the value of the equivalent resistor is an estimated value, which refers to [1].

A. Comparison of the CM-Related Quantities for Different Schemes

First, considering the proposed dual inverter with a dual winding structure, the winding neutral point voltage, i.e., the CMV comparison for different modulation schemes, is implemented, as shown in Fig. 16. In Fig. 16(a), the dual stator windings driven by the conventional SVPWM method generates a big CMV with a peak value of $\pm V_{\rm dc}/2$. Without changing any switching edges for different phase-legs, the CMV of the proposed structure has an identical waveform with that of the single inverter, and every step change of the CMV can lead to an electrostatically induced current. Fig. 16(b) shows the CMV of the SVPWM with half switching cycle interleaving. It can be seen that the peak value of the CMV reduces to $\pm V_{\rm dc}/6$; this is due to the interleaving manner that can cancel out the switching actions to a certain extent, while there still exist rising edges misaligned with falling edges,

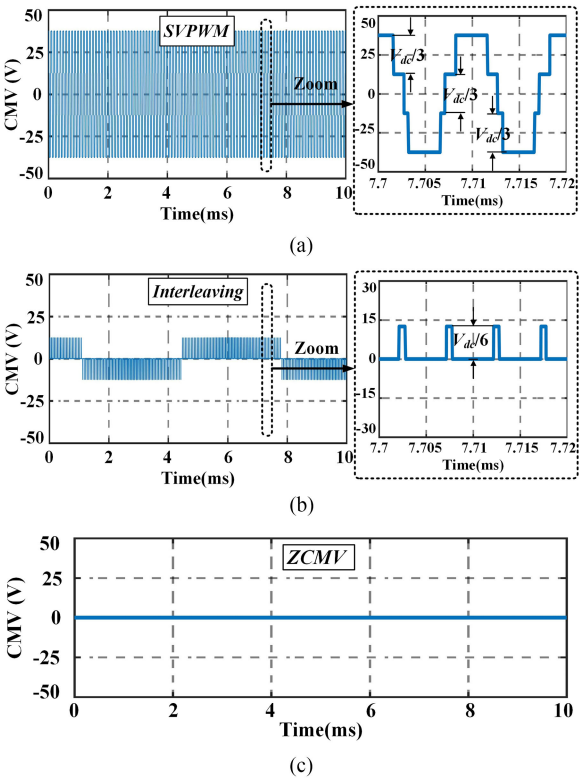

Fig. 16. CMV comparison for different modulation schemes with the proposed structure. (a) Conventional SVPWM scheme. (b) SVPWM with half switching cycle interleaving. (c) Proposed ZCMV scheme.

which lead to the discharging and charging currents generated asynchronously; thus, the leakage current cannot be avoided in this case. Fig. 16(c) shows the CMV of the proposed ZCMV scheme; it can be deduced that all the rising edges align with the corresponding falling edges to maintain the zero state of the CMV, which conforms to the theoretical analysis; thus, the discharging and charging currents can cancel each other out and lead to the elimination of the output leakage current under ideal condition. As for the original paralleled inverter with a CI structure, the CMV waveforms for different modulation schemes [22] also coincide with the corresponding results in the proposed dual winding structure, which proves that the proposed structure has no influence on the CMV, and the ZCMV scheme can eliminate the CMV under ideal condition, thereby having the best CMV suppression effect when compared with other schemes.

In addition, the leakage current comparison of different schemes is also done. Fig. 17(a) shows the leakage current of the conventional SVPWM scheme for the proposed structure. Without any different phase-legs' switching actions to cancel out the instantaneous *dv*/*dt*, the electrostatically induced leakage current generated and the six-step CMV induces six times leakage current in one switching cycle, as shown in the enlarged view. In addition, owing to a relatively big step change of the CMV $(V_{\rm dc}/3)$ in every switching action, the peak value of the leakage current reaches nearly 0.2 A in most cases. Fig. 17(b) shows the leakage current of the SVPWM with half switching cycle interleaving scheme for the proposed structure. It can be

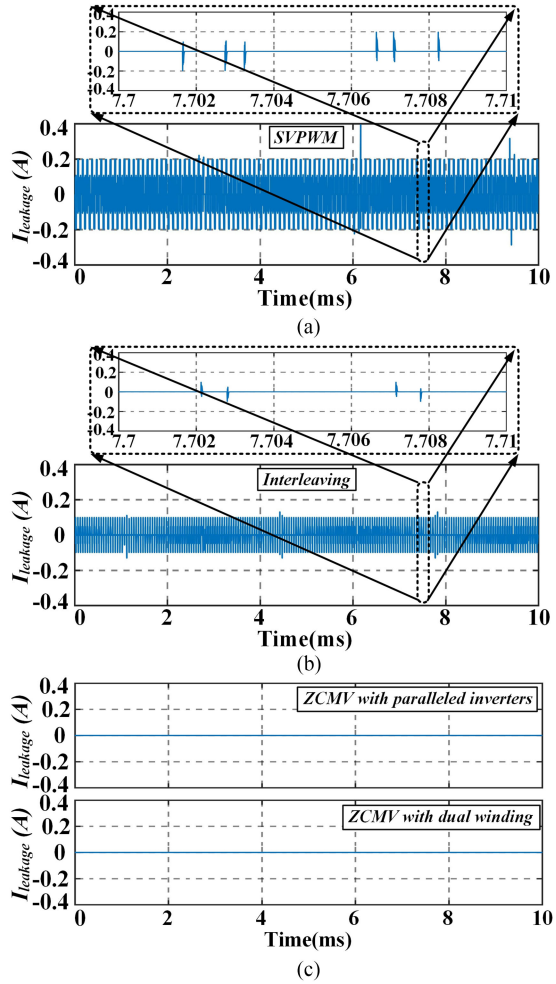

Fig. 17. Leakage current comparison for different schemes. (a) Conventional SVPWM scheme with the proposed structure. (b) SVPWM with half switching cycle interleaving with the proposed structure. (c) Proposed ZCMV scheme with the conventional and proposed structures.

found that the peak value of the leakage current reduces to 0.1 A, which is attributed to the step change reduction of the CMV $(V_{\rm dc}/6)$. Moreover, the generating time of the leakage current in one switching cycle reduces from 6 to 4, as shown in the enlarged view; this is caused by the remaining two CMV pulses' switching edges. Fig. 17(c) shows the proposed ZCMV scheme with the conventional and proposed structures. It can be clearly seen that the leakage current can be avoided in these two cases, which depends on every rising edge matching the corresponding falling edge in order to suppress the potential variation of the motor frame; thus, the leakage current can be cancelled out finally. With the above-mentioned analysis, it can be deduced that the proposed dual winding structure can maintain the effect of leakage current suppression, and the ZCMV scheme has the best performance when compared with other modulation schemes.

B. Phase Current Comparison for the ZCMV Scheme With Different Structures

For paralleled inverters with the ZCMV scheme, the voltage error for two paralleled phase-legs can be balanced in

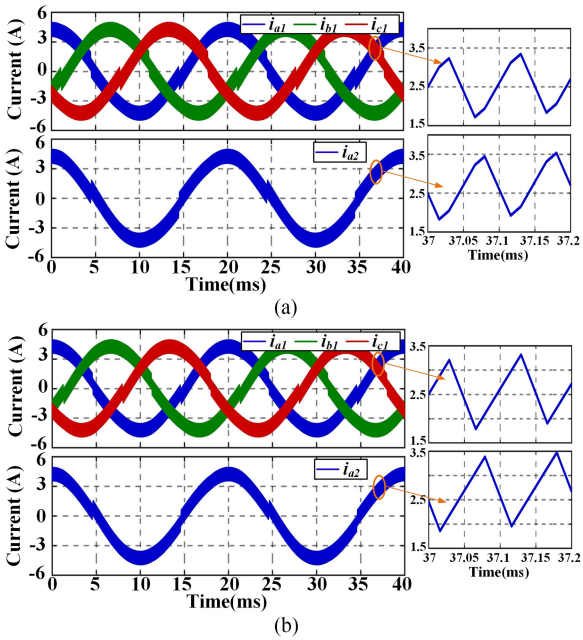

Fig. 18. Phase-leg current for different schemes. (a) Phase-leg current for the original paralleled inverter with a CI structure. (b) Phase-leg current for the proposed dual inverter with a dual winding structure.

one switching cycle, which leads to the suppression of high-frequency circulating currents [22]; thus, the fundamental phase current can be equally divided into two paralleled phase-legs under ideal condition, and the capacity of the two paralleled inverters can be fully utilized. In order to verify the characteristic of the proposed scheme, the phase current performance has been tested in the steady state with the motor working at 0.375 rated speed (at 50-Hz fundamental frequency) and half the rated load (4.15 N·m). Fig. 18 depicts the results of the original and the proposed structures. For the paralleled inverters with CIs structure, as shown in Fig. 18(a), the paralleled phase-leg currents i_{a1} and i_{a2} maintain an identical phase angle and peak value, the three-phase currents i_{a1}, i_{b1}, i_{c1} in one inverter are also symmetrical, which means the capacity of one inverter can be fully utilized and the power distribution for paralleled inverters is balanced. In addition, the current ripple of i_{a2} is with half switching cycle phaseshift when compared with i_{a1} owing to the same phaseshift in the PWM signal, as shown in the enlarged view. Fig. 18(b) shows the three phase currents in one set of stator winding and the corresponding phase A current in the other stator winding for the proposed dual inverter with a dual winding structure. It can be seen that the corresponding phase current can also be balanced and the three phase currents are also symmetrical, similar to the situation of the paralleled inverter with the CI. The only difference is the current ripple variation, which is affected by the change of circuit structure. Thus, the proposed dual inverter with a dual winding structure has no influence on the capacity of the inverter, and the dual stator winding can share the same load under ideal condition.

From the above-mentioned simulation results, it can be found that the proposed ZCMV scheme with a dual winding structure is suitable for leakage current suppression and has a similar performance as the original structure, while the CI can be excluded under this condition.

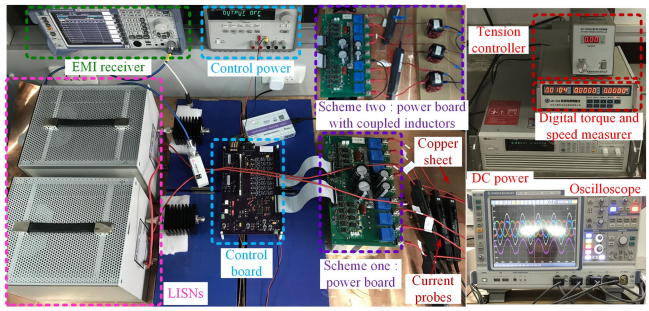

Fig. 19. Experimental platform.

TABLE IV
EXPERIMENTAL PARAMETERS

Symbol	Parameters	Value
V_{dc}	DC link voltage	75V
f_s	Switching frequency	10kHz
L_c	Main inductance of CI	0.52mH
M	Coupling coefficient of CI	0.92
L_s	Stator inductance	1.2mH
N_{ref}	Reference rotation speed	375rpm
T_e	Reference torque	4.15Nm
T_d	Dead-time	0.5μs

V. EXPERIMENTAL RESULTS AND DISCUSSION

In order to further verify the proposed method and to compare with other schemes, experiments have been done in a prototype experimental platform, as shown in Fig. 19, including the motor testbench shown in Fig. 12. The platform consists of a control board, in which the control algorithm is implemented in a DSP TMS320F28335 that can generate 12 PWMs and drive two inverters simultaneously, and a power board with two integrated power modules (IPM: 6MBP20RH060, 600 V, 20 A, FUJI) connecting the common dc-bus, which can be used as three-phase paralleled inverters or as a dual separated three-phase inverter. The platform also provides three CIs for paralleled inverter output connection, as shown in Fig. 19 for scheme two. The oscilloscope Rohde & Schwarz RTE1024 with 5-GSa/s sampling rate is utilized to capture the date and to ensure the precision of the time-domain waveform. The two line impedance stabilization networks (LISNs: NNBM 8126 A890, 0.1–150 MHz, 600 V, 100 A) are in series with the dc power and the inverters to isolate the dc power noise. Using the EMI receiver Rohde & Schwarz ESL 3, the CM EMI test can be carried out to obtain an accurate frequency spectrum characteristic. The copper sheet is utilized to provide common grounding. Other related equipment are used to provide the dc power and to add the braking torque. The common parameters used in the experiment are listed in Table IV.

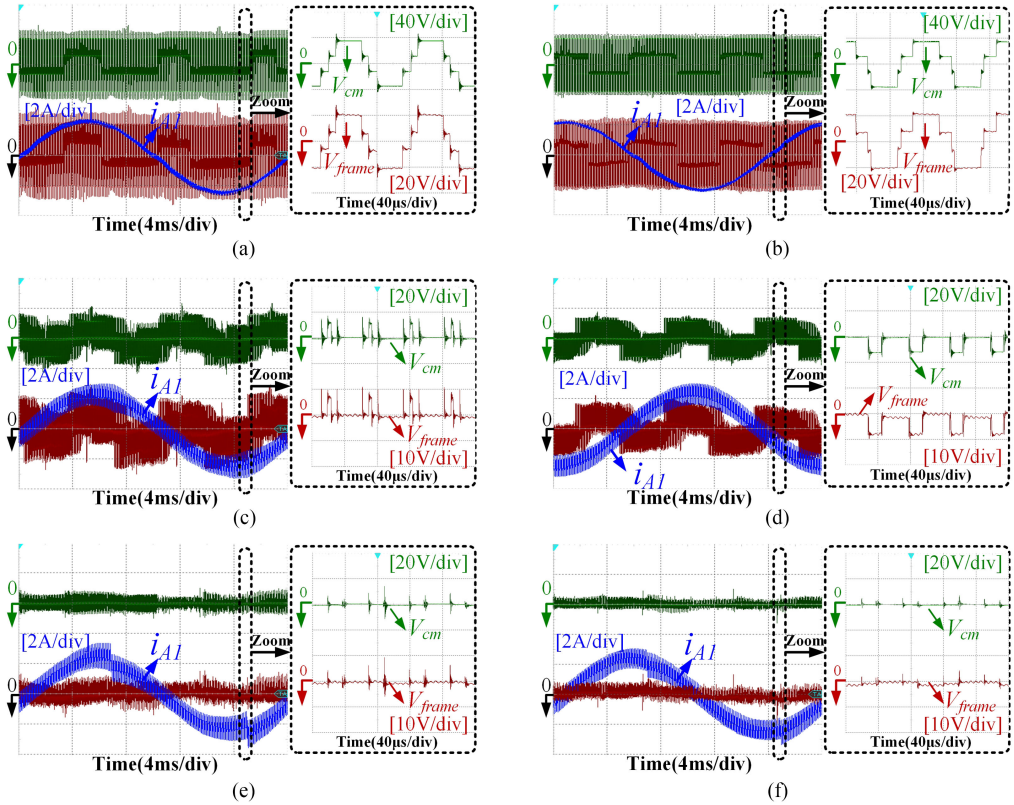

Fig. 20. CMV, motor frame voltage, and phase-leg current comparison for different schemes. (a) Conventional SVPWM for paralleled inverters with a CI. (b) Conventional SVPWM for a dual inverter with a dual winding. (c) SVPWM for paralleled inverters with a CI utilizing the interleaving manner. (d) SVPWM for a dual inverter with a dual winding utilizing the interleaving manner. (e) ZCMV for paralleled inverters with a CI. (f) ZCMV for a dual inverter with a dual winding.

A. Verification of the CMV-Related Motor Frame Voltage for Different Schemes

The frame grounding is first cancelled to measure the motor frame voltage under this condition. Based on the aforementioned stator winding configurations, the CMV and motor frame voltage of paralleled inverters with the CI and the dual inverter with dual winding schemes are tested to verify the feasibility of CI elimination. In this case, three different modulation schemes are implemented, including the conventional SVPWM, the SVPWM with interleaving, and the ZCMV. Fig. 20 shows the test results of the stator winding CMV, the motor frame voltage, and the phase-leg current to give the fundamental period reference. For the conventional SVPWM utilizing the structure of paralleled inverters with the CI and the dual inverter with a dual winding, as shown in Fig. 20(a) and (b), the CMV is a symmetric six-step wave with a peak value of $\pm V_{\rm dc}/2$, regardless of the instantaneous voltage overshoot shown in the enlarged two switching cycles view. More importantly, the motor frame voltage is directly related to the CMV, which can be almost recognized as the replica, and only the amplitude is smaller than the CMV. In addition, for the SVPWM with interleaving, the results for the two structures are depicted in Fig. 20(c) and (d). It can be found that the CMV for different structures has been reduced to $\pm V_{\rm dc}/6$, which coincides with the theoretical analysis, and the motor frame voltage also maintains the replicating relationship with the CMV. As for the ZCMV scheme with two structures, as shown in Fig. 20(e) and (f), the CMV can be further reduced when compared with the interleaving manner such that only small spikes are left. These spikes are due to the short dead-time, the switching cancellation transient process, and so on [19]. Even with some nonideal factors, the motor frame voltage can also be further reduced, which is beneficial for the leakage current suppression.

From the above-mentioned experimental results, it can be concluded that the dual inverter can directly drive the designed two-segment motor without the interference of the CMV and motor frame voltage suppression.

B. Comparison of the Leakage Current and the CM EMI for Different Modulation Schemes

In order to further test the CM leakage current and the CM EMI with different schemes, the motor frame is connected to the common copper sheet. In this case, Fig. 21 shows the CMC comparison for different structures. In Fig. 21(a), the CMC for three different modulation schemes with the conventional structure has been tested. It can be seen that the SVPWM scheme with the largest motor frame voltage has about 0.18-A peak value of CMC, regardless of some instantaneous spikes, which is the largest CMC among these three schemes. The SVPWM with interleaving scheme, which reduces but cannot eliminate the

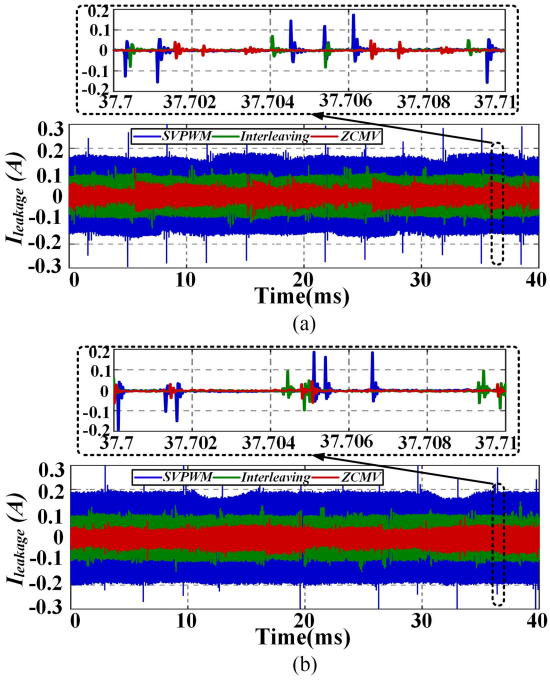

Fig. 21. CMC comparison for different schemes. (a) Conventional paralleled inverters with a CI structure for three modulation schemes. (b) Proposed dual inverter with a dual winding structure for three modulation schemes.

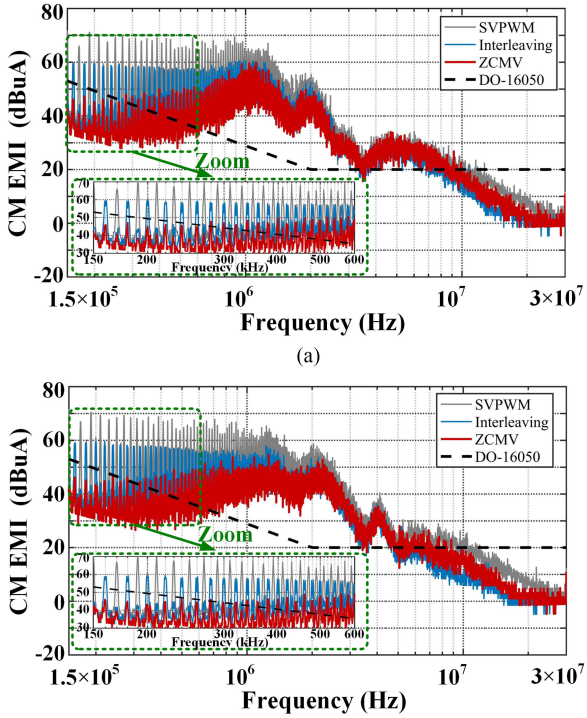

Fig. 22. CM EMI comparison for different schemes. (a) Conventional paralleled inverters with a CI structure for three modulation schemes. (b) Proposed dual inverter with a dual winding structure for three modulation schemes.

motor frame voltage, can suppress the CMC to about 0.1 A. The ZCMV scheme, which can almost eliminate the motor frame voltage, has the best CMC suppression effect, the peak value is less than 0.1 A, and the rms and average values have been reduced; this scheme has an obvious superiority in terms of EMI reduction. The left CMC is induced by the left frame voltage spike, which is caused by the nonideal factors, such as the dead-time effect, the transition process of switching actions, stator inductance asymmetry, and so on [19]. More importantly, considering the proposed structure, the CMC result has also been tested, as shown in Fig. 21(b). It can be seen that the CMC for the three modulation schemes has a similar effect as the schemes in the corresponding conventional structure, and the ZCMV scheme has the best CMC suppression effect, which proves the feasibility of the proposed scheme.

In addition, the dc-side CM EMI for different schemes has been measured and compared with the EMI standard DO-16050 [26], as shown in Fig. 22. First, the CM EMI comparison for the three different modulation schemes with the conventional structure has been performed, as shown in Fig. 22(a). It can be seen that in low EMI frequency range (150 kHz–1 MHz), the SVPWM with interleaving scheme can restrain the CM EMI near the odd switching frequency when compared with the conventional SVPWM scheme, which leads to about 10-dB EMI peak reduction. Considering the ZCMV scheme, the proposed ZCMV scheme can significantly reduce CM EMIs, regardless of the odd or even switching frequency, and the peak EMI can be further reduced to about 10 dB when compared with the SVPWM with interleaving scheme in the frequency range of 150–600 kHz. In high EMI frequency range (2–30 MHz), the influence of PWM is not dominating; thus, the three cases are close to each other. Hence, considering the requirement of the EMI standard, the ZCMV scheme can help lower the EMI filter cost and component sizes. Fig. 22(b) shows the CM EMI comparison for the proposed structure. It can be seen that the characteristic for different modulation schemes in the low EMI frequency range is similar to that of the conventional structure. Whereas, with the change of the CM loop impedance caused by the stator winding variation, the CM EMI in the high EMI frequency range for the proposed structure has different resonant frequencies, but the characteristic of the CM EMI in the high frequency range cannot obviously affect the EMI filter in this case. Thus, the ZCMV scheme for the proposed structure, which has the lowest CM EMI when compared with other modulation schemes, can also provide the function of size reduction for the CM EMI filter.

C. Comparison of the Phase Current for Different Schemes

Finally, the steady-state experiment has been carried out with the motor working at 0.375 rated speed (at 50-Hz fundamental frequency) and 0.5 rated load (4.15 N·m), and the performance of the proposed structure with the ZCMV scheme has been tested and compared with the conventional structure. The ac-side phase-leg currents have been measured, as shown in Fig. 23. Fig. 23(a) shows the ZCMV scheme utilizing the paralleled inverter with the CI structure, in which i_{A1}, i_{B1}, and i_{C1} are the three phase-leg currents for one inverter, i_{A2} is the other paralleled phase-leg current for phase A and i_A is the actual phase A current, which is the summation of i_{A1} and i_{A2}. It can

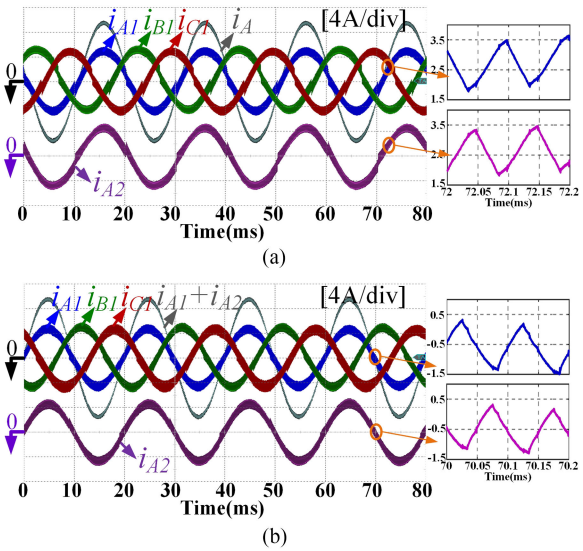

Fig. 23. Phase current comparison for different schemes. (a) ZCMV scheme utilizing the paralleled inverter with a CI structure. (b) ZCMV scheme for a dual inverter with a dual winding structure.

be found that owing to the ZCMV scheme, the fundamental phase current can be evenly distributed to paralleled phase-legs. Considering the current ripples shown in the enlarged view, the current ripple of i_{A2} is with half switching cycle phaseshift when compared with i_{A1} owing to the same phaseshift of the PWM signal, and the waveform is similar to that in the simulation result.

As for the proposed dual inverter with a dual-segment motor, the result is shown in Fig. 23(b), where i_{A1}, i_{B1}, and i_{C1} are the three phase currents for one set of stator winding, i_{A2} is the corresponding phase A current for the other stator winding, and $i_{A1} + i_{A1}$ is the equivalent phase A current. It can be found that the amplitude of corresponding phase currents is almost identical, which is about half of the designed rated current for each winding. Thus, the ZCMV scheme can also keep the corresponding phase current equally divided in the proposed dual winding structure, and this characteristic ensures the contribution to the output torque being the same for the two sets of stator windings and makes full use of the capacity of the dual inverter system. In addition, with the phaseshift of the PWM signal, the current ripple in the corresponding phase current maintains the homologous interleaved effect shown in the enlarged view, which also coincides with the simulation result, and this effect makes the performance of the equivalent phase A current similar to that of the conventional structure; hence, it can be easily deduced that the torque ripple caused by the ripple current in the phase current will not be degraded in this case.

VI. Conclusion

In this paper, a complete scheme to deal with the leakage current and CM EMIs of a motor is proposed. Comparing with the conventional scheme of paralleled inverters with CIs to drive a three-phase motor, the proposed scheme can directly drive the designed dual-segment three-phase motor, which can prevent the utilization of the CI and simplify the system structure. The following few conclusions can be derived.

1) The ZCMV modulation scheme can cooperate with the specially designed motor to cancel out the CI in a motor drive system, and the specially designed motor requires two identical groups of three-phase back EMFs.
2) With the CI cancellation in a motor drive system and by utilizing the ZCMV modulation scheme, the CMV elimination effect can be retained, which has almost no influence on the leakage current and CM EMI reduction.
3) The proposed ZCMV with a dual-segment motor can keep the corresponding phase current equally distributed in the dual winding, which ensures the same contribution to the motor output torque and makes full use of the capacity of the dual inverter system.

The simulation and experimental results all show that the proposed complete scheme is effective in reducing the leakage current and CM EMIs. Compared with the previous work on zero-CM PWM for paralleled inverters, the power density of the motor drive can be improved significantly by removing the CIs.

References

[1] S. Ogasawara and H. Akagi, "Modeling and damping of high-frequency leakage currents in PWM inverter-fed AC motor drive systems," *IEEE Trans. Ind. Appl.*, vol. 32, no. 5, pp. 1105–1114, Sep./Oct. 1996.
[2] H. Akagi and T. Shimizu, "Attenuation of conducted EMI emissions from an inverter-driven motor," *IEEE Trans. Power Electron.*, vol. 23, no. 1, pp. 282–290, Jan. 2008.
[3] J. M. Erdman, R. J. Kerkman, D. W. Schlegel, and G. L. Skibinski, "Effect of PWM inverters on AC motor bearing currents and shaft voltages," *IEEE Trans. Ind. Appl.*, vol. 32, no. 2, pp. 250–259, Mar./Apr. 1996.
[4] D. Busse, J. Erdman, R. J. Kerkman, D. Schlegel, and G. Skibinski, "Bearing currents and their relationship to PWM drives," *IEEE Trans. Power Electron.*, vol. 12, no. 2, pp. 243–252, Mar. 1997.
[5] A. Muetze, "Scaling issues for common-mode chokes to mitigate ground currents in inverter-based drive systems," *IEEE Trans. Ind. Appl.*, vol. 45, no.1, pp. 286–294, Jan./Feb. 2009.
[6] A. Muetze and C. R. Sullivan, "Simplified design of common-mode chokes for reduction of motor ground currents in inverter drives," *IEEE Trans. Ind. Appl.*, vol. 47, no. 6, pp. 2570–2577, Nov./Dec. 2011.
[7] M. L. Heldwein, L. Dalessandro, and J. W. Kolar, "The three-phase common-mode inductor: Modeling and design issues," *IEEE Trans. Ind. Electron.*, vol. 58, no. 8, pp. 3264–3274, Aug. 2011.
[8] F. Luo *et al.*, "Analysis of CM volt-second influence on CM inductor saturation and design for input EMI filters in three-phase DC-fed motor drive systems," *IEEE Trans. Power Electron.*, vol. 25, no. 7, pp. 1905–1914, Jul. 2010.
[9] M. Piazza, G. Tine, and G. Vitale, "An improved active common-mode voltage compensation device for induction motor drives," *IEEE Trans. Ind. Electron.* vol. 55, no. 4, pp. 1823–1834, Apr. 2008.
[10] S. Wang, Y. Y. Maillet, F. Wang, D. Boroyevich, and R. Burgos, "Investigation of hybrid EMI filters for common-mode EMI suppression in a motor drive system," *IEEE Trans. Power Electron.*, vol. 25, no. 4, pp. 1034–1045, Apr. 2010.
[11] A. Muetze, "On a new type of inverter-induced bearing current in large drives with one journal bearing," *IEEE Trans. Ind. Appl.*, vol. 46, no. 1, pp. 240–248, Jan./Feb. 2010.
[12] A. M. Hava and E. Ün, "A high-performance PWM algorithm for common-mode voltage reduction in three-phase voltage source inverters," *IEEE Trans. Power Electron.*, vol. 26, no. 7, pp. 1998–2008, Jul. 2011.
[13] E. Ün and A. M. Hava, "A near-state PWM method with reduced switching losses and reduced common-mode voltage for three-phase voltage source inverters," *IEEE Trans. Ind. Appl.*, vol. 45, no. 2, pp. 782–793, Mar./Apr. 2009.

[14] R. M. Tallam, R. J. Kerkman, D. Leggate, and R. A. Lukaszewski, "Common-mode voltage reduction PWM algorithm for AC drives," *IEEE Trans. Ind. Appl.*, vol. 46, no. 5, pp. 1959–1969, Sep./Oct. 2010.
[15] H. Zhang, A. von Jouanne, S. Dai, A. K. Wallace, and F. Wang, "Multilevel inverter modulation schemes to eliminate common-mode voltages," *IEEE Trans. Ind. Appl.*, vol. 36, no. 6, pp. 1645–1653, Nov./Dec. 2000.
[16] T.-K. T. Nguyen, N.-V. Nguyen, and N. R. Prasad, "Eliminated common mode voltage pulse-width modulation to reduce output current ripple for multilevel inverters," *IEEE Trans. Power Electron.*, vol. 31, no. 8, pp. 5952–5966, Aug. 2016.
[17] A. von Jauanne and H. Zhang, "A dual-bridge inverter approach to eliminating common-mode voltages and bearing and leakage currents," *IEEE Trans. Power Electron.*, vol. 14, no. 1, pp. 43–48, Jan. 1999.
[18] D. Han, C. T. Morris, and B. Sarlioglu, "Common-mode voltage cancellation in PWM motor drives with balanced inverter topology," *IEEE Trans. Ind. Electron.*, vol. 64, no. 4, pp. 2683–2688, Apr. 2017.
[19] D. Han, W. Lee, S. Li, and B. Sarlioglu, "New method for common mode voltage cancellation in motor drives: Concept, realization, and asymmetry influence," *IEEE Trans. Power Electron.*, vol. 33, no. 2, pp. 1188–1201, Feb. 2018.
[20] F. Ueda, K. Matsui, M. Asao, and K. Tsuboi, "Parallel-connections of pulsewidth modulated inverters using current sharing reactors," *IEEE Trans. Power Electron.*, vol. 10, no. 6, pp. 673–679, Nov. 1995.
[21] J. W. Kimball and M. Zawodniok, "Reducing common-mode voltage in three-phase sine-triangle PWM with interleaved carriers," *IEEE Trans. Power Electron.*, vol. 26, no. 8, pp. 1998–2008, Aug. 2011.
[22] D. Jiang, Z. Shen, and F. Wang, "Common-mode voltage reduction for paralleled inverters," *IEEE Trans. Power Electron.*, vol. 33, no. 5, pp. 3961–3974, May 2018.
[23] G. Gohil *et al.*, "Modified discontinuous PWM for size reduction of the circulating current filter in parallel interleaved converters," *IEEE Trans. Power Electron.*, vol. 30, no. 7, pp. 3457–3470, Jul. 2015.
[24] Y. Murai, T. Kubota, and Y. Kawase, "Leakage current reduction for a high-frequency carrier inverter feeding an induction motor," *IEEE Trans. Ind. Appl.*, vol. 28, no. 4, pp. 858–863, Jul./Aug. 1992.
[25] K. Zhou and D. Wang, "Relationship between space-vector modulation and three-phase carrier-based PWM: A comprehensive analysis," *IEEE Trans. Ind. Electron.*, vol. 49, no. 1, pp. 186–196, Feb. 2002.
[26] *Environmental Conditions and Test Procedures for Airborne Equipment*, DO-160E, RTCA Inc., Washington, DC, USA, 2004.

Zewei Shen (S'17) was born in Hubei, China, in 1990. He received the B.S. degree in automation from the Department of Automation, Huazhong University of Science and Technology, Wuhan, China, in 2012. He is currently working toward the Ph.D. degree in electrical engineering at the Huazhong University of Science and Technology.

His research interests include paralleled converters and high power density motor drives.

Dong Jiang (S05'–M12'–SM16') received the B.S. and M.S. degrees in electrical engineering from Tsinghua University, Beijing, China, in 2005 and 2007, respectively. He began the Ph.D. degree study at the Center for Power Electronics Systems, Virginia Tech, Blacksburg, VA, USA, in 2007 and was transferred to the University of Tennessee, Knoxville, TN, USA, with his advisor in 2010. He received the Ph.D. degree from the University of Tennessee in December 2011.

From January 2012 to July 2015, he was a Senior Research Scientist/Engineer with the United Technologies Research Center, East Hartford, CT, USA. Since July 2015, he has been a Professor with the Huazhong University of Science and Technology, Wuhan, China. He has authored or coauthored more than 40 published IEEE journal and conference papers. His research interests include power electronics and motor drives.

Dr. Jiang was the recipient of two Best Paper Awards in IEEE conferences. He is an Associate Editor for the IEEE TRANSACTIONS ON INDUSTRY APPLICATIONS.

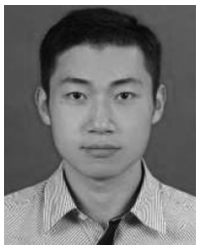

Tianjie Zou (S'15) was born in Hubei, China, in 1991. He received the B.E.E. degree in electrical and electronic engineering from the Huazhong University of Science and Technology, Wuhan, China, in 2013, where he is currently working toward the Ph.D. degree in electrical engineering.

His research interests include design, analysis, and intelligent control of PM machines.

Ronghai Qu (S'01–M'02–SM'05–F'18) was born in China. He received the B.E.E. and M.S.E.E. degrees in electrical engineering from Tsinghua University, Beijing, China, in 1993 and1996, respectively, and the Ph.D. degree in electrical engineering from the University of Wisconsin-Madison, Madison, WI, USA, in 2002.

In 1998, he was a Research Assistant with the Wisconsin Electric Machines and Power Electronics Consortium. He became a Senior Electrical Engineer with Northland, a Scott Fetzer Company, in 2002. Since 2003, he has been with the Electrical Machines and Drives Laboratory, General Electric (GE) Global Research Center, Niskayuna, NY, USA, as a Senior Electrical Engineer. Since 2010, he has been a Professor with the Huazhong University of Science and Technology, Wuhan, China. He has authored over 50 published technical papers and is the holder of over 40 patents/patent applications.

Dr. Qu is a full member of Sigma Xi. He has been the recipient of several awards from the GE Global Research Center since 2003, including the Technical Achievement and Management Awards. He was also the recipient of the 2003 and 2005 Best Paper Awards, Third Prize, from the Electric Machines Committee of the IEEE Industry Applications Society at the 2002 and 2004 IAS Annual Meeting, respectively.